J Clust Sci (2009) 20:601–609
DOI 10.1007/s10876-009-0266-1

ORIGINAL PAPER

Diversity of Functionalized Germanium Zintl Clusters: Syntheses and Theoretical Studies of $[Ge_9PdPPh_3]^{3-}$ and $[Ni@(Ge_9PdPPh_3)]^{2-}$

Zhong-Ming Sun · Ya-Fan Zhao · Jun Li · Lai-Sheng Wang

Received: 29 April 2009 / Published online: 4 August 2009

Abstract A new Zintl cluster $[Ge_9PdPPh_3]^{3-}$ has been isolated as (2,2,2-crypt)K^+ salt through the reaction of K_4Ge_9 and $Pd[PPh_3]_4$ in ethylenediamine solutions and characterized via single-crystal X-ray crystallography. The as-prepared bimetallic $[Ge_9PdPPh_3]^{3-}$ cluster could successfully trap a nickel atom to form a trimetallic cluster $[Ni@(Ge_9PdPPh_3)]^{2-}$. The coordination of Ge_9^{4-} by $PdPPh_3$ induces a one-electron oxidation and encapsulation of the Ni atom into the Ge_9^{3-} cage leads to a further one-electron oxidation and a geometry transformation from C_{4v} (*nido*) to C_{3v} (*closo*).

Keywords Germanium Cluster · Stannaspherene · Crystal structure · Zintl ion

Electronic supplementary material The online version of this article (doi:10.1007/s10876-009-0266-1) contains supplementary material, which is available to authorized users.

Z.-M. Sun · L.-S. Wang (✉)
Department of Physics, Washington State University, 2710 University Drive, Richland, WA 99354, USA
e-mail: ls.wang@pnl.gov

Z.-M. Sun · L.-S. Wang
Chemical and Materials Sciences Division, Pacific Northwest National Laboratory, MS K8-88, Post Office Box 999, Richland, WA 99352, USA

Y.-F. Zhao · J. Li (✉)
Department of Chemistry and Key Laboratory of Organic Optoelectronics and Molecular Engineering of Ministry of Education, Tsinghua University, Beijing 100084, China
e-mail: junli@tsinghua.edu.cn

Introduction

Deltahedral clusters of group-14 elements have attracted significant attention due to their interesting structural diversities and rich chemistry. A number of discrete, oligomeric, and functionalized clusters have been synthesized by the reactions of the well-known Zintl ion E_9^{x-} (E = Ge, Sn, Pb, x = 2–4) with main-group and transition-metal compounds, opening new possibilities for chemical reactions and the development of cluster-assembled nano-scaled materials [1–3]. For instance, an empty *closo* cluster Pb_{10}^{2-} has been isolated after oxidation of Pb_9^{4-} by an Au(I) compound in ethylenediamine (en) solution [4]. A major research objective of cluster science is to discover highly stable clusters, which may be used as building blocks for cluster-assembled nanomaterials. Recently, a 12-atom Sn cluster (Sn_{12}^{2-}), named stannaspherene, has been found to be a highly stable icosahedral cage during gas-phase photoelectron spectroscopy (PES) experiments [5]. Theoretical calculations show that stannaspherene has a diameter of 6.1 Å, large enough to entrap a foreign atom. It has been shown that indeed all transition-metals and f-block elements can be doped inside stannaspherene, giving rise to a whole new class of highly stable endohedral clusters [6]. During ongoing studies, we have further shown that Pb_{12}^{2-} (plumbaspherene) [7, 8] and Ge_{12}^{2-} (germaspherene)[1] are also highly stable icosahedral cage clusters in the gas phase and should be able to trap a variety of foreign atoms. Interestingly, a series of endohedral cage anions, $M@Pb_{12}^{2-}$ (M = Ni, Pd, Pt), have been synthesized through chemical reactions of K_4Pb_9 and ML_4 (M = Ni, Pd, Pt; L = PPh_3) and crystallized as (2,2,2-crypt)K^+ salts [9, 10, 11]. Other examples of group 14 Zintl ions centered by a transition metal atom include $Ni@Ge_9^{3-}$ [12] $Pd_2@E_{18}^{4-}$ (E = Ge, Sn) [13–15], $Pt_2@Sn_{17}^{4-}$ [16], $Ni@Pb_{10}^{2-}$[9, 10, 11], $Cu@E_9^{3-}$ (E = Sn, Pb) [17], and recently reported $M@Ge_{10}^{3-}$ (M = Fe, Co) [18, 19]. It is worthy to note that the $Pd_2@E_{18}^{4-}$ clusters can be viewed as the fusion of two endohedral $Pd@E_{12}^{2-}$ clusters by removing two E_3 triangles at the connecting interface.

From our previous PES and computational studies, E_{12}^{2-} (E = Ge, Sn, Pb) dianions are electronically rather stable. We are therefore interested in the syntheses and structural characterization of empty E_{12}^{2-} cages and their endohedral derivatives, which are expected to be stable solution species and may be crystallized with appropriate counter ions. During our attempt to synthesize the endohedral $Pd@Ge_{12}^{2-}$ cluster, we obtained, however, a new bimetallic $Ge_9PdPPh_3^{3-}$ (**1**) cluster. Additionally, we found that $Ge_9PdPPh_3^{3-}$ can further react with $Ni(PPh_3)_4$ to form a new endohedral cluster $[Ni@(Ge_9PdPPh_3)]^{2-}$ (**2**), which is a trimetallic derivative of the group-14 E_9^{x-} Zintl clusters. The reactions from Ge_9^{4-} to **1** and **2** represent an intriguing consecutive oxidation of the cluster. In this paper we report their syntheses, experimental and theoretical characterizations.

[1] Different from Sn_{12}^{2-}, Ge_{12}^{2-} has two energetically close isomers, a low-symmetry C_1 isomer and an icosahedral isomer. The icosahedral Ge_{12}^{2-} cage can trap certain foreign atoms with relatively small sizes due to its smaller cage diameter compared with Sn_{12}^{2-} and Pb_{12}^{2-}.

Experimental Section

All manipulations were carried out under a nitrogen atmosphere using standard Schlenk-line and glovebox techniques. The K_4Ge_9 precursor was synthesized from a stoichiometric mixture of the elements of K (Strem) and Ge (Strem) sealed in a Nb tube, which was heated at 950 °C for 12 hours in a quartz tube furnace under argon flow. Ethylenediamine (99+%, Acros) was commercially purchased and distilled over sodium, collected and freshly used. 2,2,2-crypt (Acros, 98%), $Pd(PPh_3)_4$ (Alfa-Aesar, 99%), and $Ni(PPh_3)_4$ (Aldrich, 99%) were used as received. A mixture of K_4Ge_9 (81.0 mg, 0.10 mmol) and 2,2,2-crypt (157 mg, 0.40 mmol) was dissolved in en (5 mL) in a 7-mL vial inside a N_2-filled glovebox and stirred for 10 min, resulting in a red–brown solution. $Pd(PPh_3)_4$ (116 mg, 0.10 mmol) was then added as a solid and the mixture was stirred for 2 h. The resulted dark brown solution was equally divided into two different vials. In vial 1, the solution was filtered through compact glass wool and layered with toluene. Large, nicely shaped needle-like dark brown crystals of $[K(2,2,2\text{-crypt})]_3(Ge_9Pd\text{-}PPh_3)\cdot en$ were yielded 3 days later (68 mg, ca. 58%, crystalline yield). In vial 2, the solution was added by $Ni(PPh_3)_4$ (40 mg, 0.036 mmol) as a solid and the mixture was stirred for additional 1 h, the final solution was filtered through a tightly packed glass wool and layered by toluene. Nicely shaped brick red–brown crystals of $[K(2,2,2\text{-crypt})]_2(Ni@Ge_9Pd\text{-}PPh_3)\cdot en$ were observed on the vial wall 3 days later (16 mg, ca. 23%, crystalline yield). Several crystals were picked for EDX analysis, which indicated the presence of Ni, Pd and Ge with an average atomic ratio of 1.2:1.0:8.5 [supporting information, Fig. S1]. Data sets were collected on a Bruker Proteum diffractometer with a CCD area detector at 223 K with Cu Kα radiation. Crystals (sizes around $0.35 \times 0.10 \times 0.10$ mm^3 for **1**, $0.10 \times 0.08 \times 0.08$ mm^3 for **2**) were selected under high vacuum grease, mounted on crystal loops, and positioned in a cold N_2 stream in the diffractometer. The structures were solved using direct methods (SHELXTL) and refined by least-squares methods with atomic coordinates and anisotropic thermal parameters [20]. CCDC 676339 & 676340 contain the supplementary crystallographic data for this paper. These data can be obtained free of charge from CCDC via www.ccdc.cam.ac.uk/data_request/cif.

Theoretical Calculations

We performed quasi-relativistic density functional calculations on the Ge_9^{4-}, Ge_9Pd^{x-} (x = 2, 4), $Ge_9PdPR_3^{x-}$ (x = 3, 4), and $Ni@Ge_9PdPR_3^{2-}$ (R = H, Ph) clusters using Amsterdam Density Functional code (ADF 2006.01) [21–23]. The generalized gradient approach of Perdew-Wang 1991 (PW91) was employed with uncontracted Slater basis sets with quality of triple-zeta plus two polarization functions (TZ2P) [24, 25]. The frozen core approximation was applied to the $[1s^2]$ atomic core of C, $[1s^2\text{–}2p^6]$ of P, and $[1s^2\text{–}3d^{10}]$ of Ge and Pd, with the rest of the electrons explicitly treated variationally [26]. The zero-order-regular approximation (ZORA) was used to account for the scalar and spin-orbit coupling relativistic effects [27]. The geometries were fully optimized with inclusion of the scalar

relativistic effects and single-point spin-orbit coupling calculations were performed with these optimized geometries. Vibrational frequency calculations were accomplished to verify the nature of the clusters on the potential energy surfaces. The optimized bond lengths and bond angles are in good agreement with the crystallographic values and optimized coordinates of the model clusters $Ge_9PdPh_3^{3-}$ and $Ni@Ge_9PdPh_3^{2-}$ are listed in Table S1.

Results and Discussion

$Ge_9PdPPh_3^{3-}$ (Fig. 1a) was crystallized as a (2,2,2-crypt)K^+ salt in an ethylenediamine solution via the reaction of K_4Ge_9 and $Pd(PPh_3)_4$. By further addition of $Ni(PPh_3)_4$, a new compound $[Ni@(Ge_9PdPPh_3)]^{2-}$ was also crystallized. The crystal structures of the two clusters have been confirmed by single-crystal X-ray diffraction. A summary of the crystallographic data is given in Table 1, and selected bond distances are listed in Table 2.

Figure 1 shows the structures of **1** and **2**. The anion $Ge_9PdPPh_3^{3-}$ features a bicapped antiprismatic cluster, where one of the capping vertexes is occupied by a Pd atom coordinated by a PPh_3 ligand. The formation of **1** can be viewed as the attachment of a neutral $PdPPh_3$ fragment to the open square side of a *nido*-Ge_9^{3-} ion. It is structurally similar to the known Zintl ions, such as $E_9M(CO)_3^{4-}$ (E = Sn, Pb; M = Cr, Mo, W) [28, 29], E_9ZnR^{3-} (E = Ge, Sn, Pb; R = Ph, Mes, ^{i}Pr) [30, 31], Ge_9NiCO^{3-} [32–34], and Pb_{10}^{2-} [4]. The Pd–Ge distances to the capped square

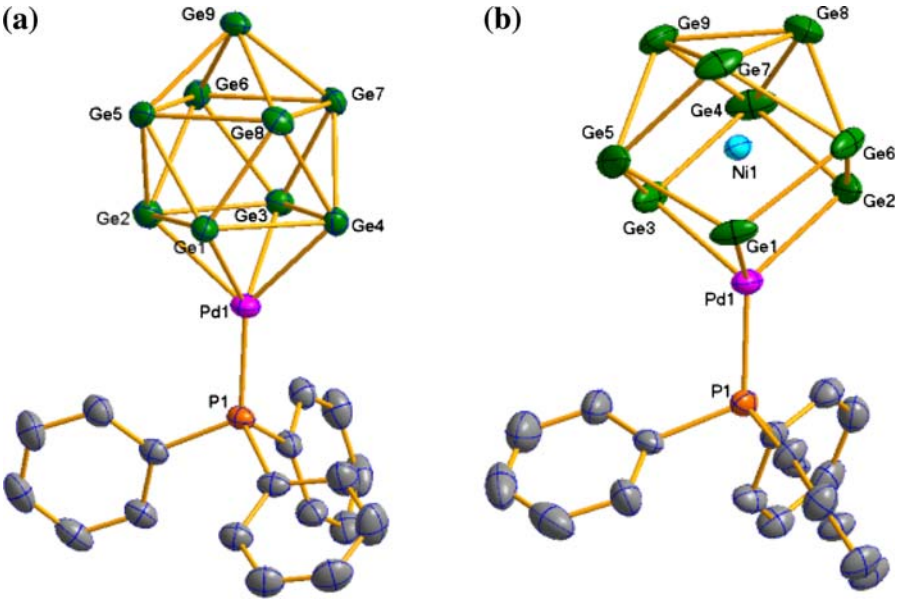

Fig. 1 **a** Structure of $Ge_9PdPPh_3^{3-}$ (**1**) in $[K(2,2,2\text{-crypt})]_3$ (Ge_9PdPPh_3)·en and **b** $Ni@Ge_9PdPPh_3^{2-}$ (**2**) in $[K(2,2,2\text{-crypt})]_2$($Ni@Ge_9PdPPh_3$)·en. Thermal ellipsoids are drawn in 30% probability

Table 1 Summary of cell parameters, data collection and structural refinements

Empirical formula	$C_{74}H_{131}K_3N_8O_{18}Ge_9Pd$	$C_{56}H_{95}K_2N_6O_{12}PGe_9NiPd$
fw	2342.83	1971.97
Space group	Triclinic, P-*1* (No. 2)	
a/Å	13.830(3)	12.992(3)
b/Å	15.970(3)	13.267(3)
c/Å	25.720(5)	23.812(5)
α, deg	100.89	79.02(3)
β, deg	91.05(3)	74.29(3)
γ, deg	113.20	82.96(3)
V, Å^3	5100.1(2)	3867.6(1)
Z	2	
D_{calcd}, g cm^{-3}	1.516	1.693
Temp, K		223(2)
λ(Å)	Cu K_α, 1.54178	
μ, mm^{-1}	6.062	7.557
F(000)	2362	1968
hkl ranges	(−16, 15), (−17, 18), (−30, 29)	±13, (−10, 14), (−25, 26)
Reflections collected/unique	40883/16626	11342/8159
GOF on F^2	1.106	1.095
R1, *wR2* ($I > 2\sigma(I)$)[a]	0.0511/0. 1550	0.0711/0.1686
R1, *wR2*(all data)	0.0577/0. 1657	0.1061/0.1850
Largest diff. peak and hole (e. Å^{-3})	1.970 and −1.163	1.683 and −1.154

$R1 = \sum||Fo| - |Fc||/\sum|Fo|$, $wR2 = \{\sum w[(Fo)^2 - (Fc)^2]^2/\sum w[(Fo)^2]^2\}^{1/2}$

range from 2.544 to 2.644 Å (Fig. 1a), which are slightly shorter than those in the endohedral complex $Pd_2@Ge_{18}^{4-}$ (2.605–2.634 Å) [13]. The Ge–Ge distances within the square (Ge1, 2, 3, 4) capped by the Pd atom average 2.709 Å, whereas the Ge–Ge distances within the other square (Ge5, 6, 7, 8) average 2.831 Å. Overall, the Ge_9 core in **1** has pseudo-C_{4v} symmetry, only slightly distorted by the capping of the $PdPPh_3$ fragment.

The trimetallic $[Ni@(Ge_9PdPPh_3)]^{2-}$ cluster **2** (Fig. 1b) can be viewed as the encapsulation of a nickel atom in the cage of **1** followed by a geometry transformation of the Ge_9 core from C_{4v} to D_{3h} symmetry, which is necessary for the 20-electron $[Ge_9]^{2-}$ to maximize the interaction between the endohedral Ni and the more spherical D_{3h} cage. Due to the coordination of PPh_3 on Pd, the actual symmetry of **2** is pseudo-C_{3v}, isostructural with $[Pt@(Sn_9PtPPh_3)]^{2-}$ and $[Ni@(Ge_9NiL)]^{x-}$ (L = CO, PPh_3, en, and $PhC\equiv C^-$, $x = 2$, 3) [32–34]. The distances from the centered nickel atom to Ge atoms range from 2.319 to 2.444 Å, comparable to those in the $[Ni@(Ge_9Ni–L)]^{x-}$ clusters. The Ni–Pd bond length of 2.492 Å is slightly larger than the corresponding Ni–Ni bonds of 2.359 and 2.382 Å in $[Ni@(Ge_9NiPPh_3)]^{2-}$ and $[Ni@(Ge_9NiC\equiv CPh)]^{3-}$, respectively, but much shorter than the Pt–Pt bond (2.697 Å) in $[Pt@(Sn_9PtPPh_3)]^{2-}$. The distances from the capping Pd atom to the three Ge atoms are nearly identical and lie in a very narrow range of 2.487–2.506 Å, slightly shorter than the Pd–Ge bonds in **1**.

Table 2 Selected bond lengths (Å) for compounds $[K(2,2,2\text{-crypt})]_3(Ge_9Pd\text{-}PPh_3)\cdot en$ and $[K(2,2,2\text{-crypt})]_2(Ni@Ge_9Pd\text{-}PPh_3)\cdot en$

$[K(2,2,2\text{-crypt})]_3(Ge_9Pd\text{-}PPh_3)\cdot en$			
Pd(1)–P(1)	2.237(1)	Pd(1)–Ge(1)	2.5440(9)
Pd(1)–Ge(3)	2.5790(9)	Pd(1)–Ge(4)	2.582(2)
Pd(1)–Ge(2)	2.644(1)	Ge(1)–Ge(8)	2.564(2)
Ge(1)–Ge(5)	2.605(1)	Ge(1)–Ge(2)	2.700(1)
Ge(1)–Ge(4)	2.703(1)	Ge(2)–Ge(6)	2.604(1)
Ge(2)–Ge(5)	2.618(1)	Ge(2)–Ge(3)	2.723(1)
Ge(3)–Ge(7)	2.570(1)	Ge(3)–Ge(6)	2.620(1)
Ge(3)–Ge(4)	2.757(1)	Ge(4)–Ge(7)	2.622(1)
Ge(4)–Ge(8)	2.630(1)	Ge(5)–Ge(9)	2.561(1)
Ge(5)–Ge(6)	2.786(1)	Ge(5)–Ge(8)	2.866(1)
Ge(6)–Ge(9)	2.580(1)	Ge(6)–Ge(7)	2.865(1)
Ge(7)–Ge(9)	2.602 (1)	Ge(7)–Ge(8)	2.817(1)
Ge(8)–Ge(9)	2.604(1)		
$[K(2,2,2\text{-crypt})]_2(Ni@Ge_9Pd\text{-}PPh_3)\cdot en$			
Pd(1)–P(1)	2.235(3)	Pd(1)–Ge(3)	2.487(2)
Pd(1)–Ni(1)	2.492(2)	Pd(1)–Ge(1)	2.494(2)
Pd(1)–Ge(2)	2.506(2)	Ni(1)–Ge(1)	2.319(3)
Ni(1)–Ge(3)	2.339(2)	Ni(1)–Ge(2)	2.343(3)
Ni(1)–Ge(6)	2.427(2)	Ni(1)–Ge(4)	2.435(3)
Ni(1)–Ge(8)	2.437(2)	Ni(1)–Ge(9)	2.441(2)
Ni(1)–Ge(7)	2.441(3)	Ni(1)–Ge(5)	2.444(3)
Ge(1)–Ge(6)	2.614(4)	Ge(1)–Ge(5)	2.633(3)
Ge(2)–Ge(4)	2.598(3)	Ge(2)–Ge(6)	2.601(3)
Ge(3)–Ge(4)	2.599(4)	Ge(3)–Ge(5)	2.607(4)
Ge(4)–Ge(8)	2.686(4)	Ge(4)–Ge(9)	2.762(3)
Ge(5)–Ge(9)	2.713(3)	Ge(5)–Ge(7)	2.740(4)
Ge(6)–Ge(8)	2.711(3)	Ge(6)–Ge(7)	2.763(3)
Ge(7)–Ge(9)	2.594(3)	Ge(7)–Ge(8)	2.644(4)
Ge(8)–Ge(9)	2.625(3)		

One of the interesting features of **1** and **2** are their 21 and 20 skeletal electrons, respectively. Similar phenomenon has also been observed in other clusters, such as Ge_9NiCO^{3-} (21e), $[Pt@(Sn_9PtPPh_3)]^{2-}$ (20e), and $[Ni@(Ge_9Ni\text{–}L)]^{x-}$ (L = PhC≡ C^-, CO; 20e) [32–34]. As Ge is isolobal and valently isoelectronic to the BH group, the Ge_9^{x-} clusters follow Wade's skeletal electron counting rules [35]. Based on Wade's rule, the 22-electron Ge_9^{4-} cluster and the 20-electron Ge_9^{2-} cluster should adopt a *nido* (C_{4v}) and *closo* (D_{3h}) structure, respectively. Accordingly, **1** and **2** should have pseudo-C_{4v} and pseudo-C_{3v} symmetry, respectively, as indeed observed experimentally. However, **1** only has 21 skeletal electrons, indicating the 22e cluster is readily oxidized.

Table 3 Calculated HOMO-LUMO gaps of Ge_9^{4-}, Ge_9Pd^{4-}, $Ge_9PdPR_3^{4-}$, $Ni@Ge_9Pd^{2-}$, and $Ni@Ge_9PdPR_3^{2-}$, (R=H, Ph)

	Sym.	SR	SO
Ge_9^{4-}	C_{4v}	1.53	1.51
Ge_9Pd^{4-}	C_{4v}	1.23	1.20
$Ge_9PdPH_3^{4-}$	"C_{4v}"	0.86	0.85
$Ge_9PdPPh_3^{4-}$	"C_{4v}"	0.18	0.18
$Ni@Ge_9Pd^{2-}$	C_{4v}	0.56	0.54
$Ni@Ge_9Pd^{2-}$	C_{3v}	0.87	0.87
$Ni@Ge_9PdPH_3^{2-}$	"C_{3v}"	1.57	1.56
$Ni@Ge_9PdPPh_3^{2-}$	"C_{3v}"	0.80	0.79

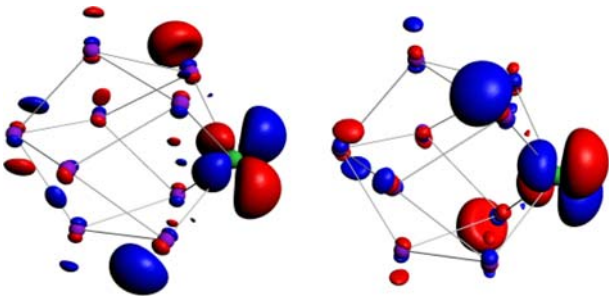

Fig. 2 The calculated highest occupied molecular orbital of Ge_9Pd^{4-}

To elucidate the stability and the electronic structure of **1** and **2**, we performed quasi-relativistic density functional calculations on the Ge_9^{4-}, Ge_9Pd^{x-} ($x = 2, 4$), $Ge_9PdPR_3^{x-}$ ($x = 3, 4$), and $Ni@Ge_9PdPR_3^{2-}$ (R = H, Ph) clusters using the PW91 generalized gradient approach implemented in ADF 2006.01 [21–25]. The geometries were fully optimized at the level of scalar relativistic zero-order regular approximation (ZORA) [26]. The optimized bond lengths and bond angles are in good agreement with the crystallographic values.

The calculated scalar relativistic (SR) and spin-orbit (SO) coupled HOMO-LUMO energy gaps (ΔE_{HL}) of these clusters are listed in Table 3. Clearly the *nido*-Ge_9^{4-} cluster has large ΔE_{HL}, which is consistent with the existence of various stable A_4Ge_9 (A = alkali metals) compounds. The HOMO-LUMO gap decreases when Pd or $PdPR_3$ occupies the open square of the *nido*-Ge_9^{4-} cluster, due to the interaction of the Pd $4d^{10}$ orbitals and the out-pointing lone pairs of Ge_9. Bonding analysis indicates that the HOMO of Ge_9Pd^{4-} is nearly non-bonding (Fig. 2), due to the cancellation of the weak-bonding within Ge_9 and antibonding between the Ge_9 and Pd orbitals. The non-bonding nature of the highest occupied orbitals is remarkable in the $Ge_9PdPR_3^{4-}$ (R = H, Ph) clusters, which have much smaller HOMO-LUMO gaps and are easily oxidized. This explains why **1** violates the Wade's rule to possess 21 rather than 22 electrons. Indeed the calculations show a spin 1/2 ground state for **1**.

Theoretical calculations reveal that when Ni atom is inserted into the C_{4v} structure of Ge_9Pd^{2-}, the HOMO-LUMO gap is quite small and the structure in fact becomes a transition state. Starting from this structure, geometry optimization without symmetry restriction leads to the C_{3v} structure of $Ni@Ge_9Pd^{2-}$ with a larger HOMO-LUMO gap and significant energy lowering (0.54 eV), explaining why experimentally **2** is observed.

In conclusion, a new Zintl cluster, $Ge_9PdPPh_3^{3-}$, with 21 electrons has been synthesized. Reaction of **1** with $Ni(PPh_3)_4$ leads to the formation of a 20-electron cluster, $Ni@Ge_9PdPPh_3^{2-}$. We have shown that the coordination of Ge_9^{4-} by $PdPPh_3$ induces a one-electron oxidation and encapsulation of the Ni atom into the $Ge_9PdPPh_3^{3-}$ cage leads to a further one-electron oxidation and a geometry transformation of Ge_9 from pseudo-C_{4v} (*nido*) to pseudo-C_{3v} (*closo*) structure.

Ackowledgement We thank Dr. Mike R. Thompson and Dr. Angel Ugrinov for help with the X-ray diffraction measurements and valuable discussions. The experimental work was supported by the National Science Foundation (DMR-0503383) and partially by the Petroleum Research Fund (PRF# 46275-AC6) administered by the American Chemical Society and performed at EMSL, a national scientific user facility sponsored by DOE[1]s Office of Biological and Environmental Research and located at Pacific Northwest National Laboratory, operated for DOE by Battelle. Acknowledgment is also made to the Donors of the American Chemical Society Petroleum Research Fund for partial support of this research. The theoretical work, supported by NKBRSF (2006CB932305, 2007CB815200) and NNSFC (20525104) in China, were performed using a HP Itanium2 cluster at Tsinghua National Laboratory for Information Science and Technology.

References

1. J. D. Corbett (2000). *Angew. Chem. Int. Ed.* **39**, 670.
2. S. C. Sevov and J. M. Goicoechea (2006). *Organometallics* **25**, 5678.
3. T. F. Fässler and S. D. Hoffmann (2004). *Angew. Chem. Int. Ed.* **43**, 6242.
4. A. Spiekermann, S. D. Hoffmann, and T. F. Fässler (2006). *Angew. Chem. Int. Ed.* **45**, 3459.
5. L. F. Cui, X. Huang, L. M. Wang, D. Y. Zubarev, A. I. Boldyrev, J. Li, and L. S. Wang (2006). *J. Am. Chem. Soc.* **128**, 8390.
6. L. F. Cui, X. Huang, L. M. Wang, J. Li, and L. S. Wang (2007). *Angew. Chem. Int. Ed.* **46**, 742.
7. L. F. Cui, X. Huang, L. M. Wang, J. Li, and L. S. Wang (2006). *J. Phys. Chem. A* **110**, 10169.
8. L. F. Cui and L. S. Wang (2008). *Int. Rev. Phys. Chem.* **27**, 139.
9. E. N. Esenturk, J. Fettinger, Y. F. Lam, and B. Eichhorn (2004). *Angew. Chem. Int. Ed.* **43**, 2132.
10. E. N. Esenturk, J. Fettinger, B. Eichhorn (2005). Chem. Commun. 247.
10. E. N. Esenturk, J. Fettinger, and B. Eichhorn (2006). *J. Am. Chem. Soc.* **128**, 9178.
12. J. M. Goicoechea and S. C. Sevov (2005). *Angew. Chem. Int. Ed.* **44**, 4026.
13. J. M. Goicoechea and S. C. Sevov (2005). *J. Am. Chem. Soc.* **127**, 7676.
14. Z. M. Sun, H. Xiao, J. Li, and L. S. Wang (2007). *J. Am. Chem. Soc.* **129**, 9560.
15. F. S. Kocak, P. Zavalij, Y. F. Lam, and B. W. Eichhorn (2008). *Inorg. Chem.* **47**, 3515.
16. B. Kesanli, J. E. Halsig, P. Zavalij, J. Fettinger, Y. F. Lam, and B. Eichhorn (2007). *J. Am. Chem. Soc.* **129**, 4567.
17. S. Scharfe, T. F. Fassler, S. Stegmaier, S. D. Hoffman, and K. Ruhland (2008). *Chem. Eur. J.* **14**, 4479.
18. J. Q. Wang, S. Stegmaier, and T. F. Fässler (2009). *Angew. Chem. Int. Ed.* **48**, 1998.
19. B. B. Zhou, M. S. Denning, D. L. Kays, and J. M. Goicoechea (2009). *J. Am. Chem. Soc.* **131**, 2802.
20. G. M. Sheldrick, SHELXTL (1998). Crystallographic Software Package, version 5.1; Bruker-AXS; Madison, WI.

21. ADF 2006.01, SCM, Theoretical Chemistry, Vrije Universiteit, Amsterdam, The Netherlands (http://www.scm.com).
22. G. te Velde, F. M. Bickelhaupt, S. J. A. van Gisbergen, C. Fonseca Guerra, E. J. Baerends, J. G. Snijders, and T. Ziegler (2001). *J. Comput. Chem.* **22**, 931.
23. C. Fonseca Guerra, J. G. Snijders, G. te Velde, and E. J. Baerends (1998). *Theor. Chem. Acc.* **99**, 391.
24. J. P. Perdew and Y. Wang (1992). *Phys. Rev. B* **45**, 13244.
25. E. van Lenthe and E. J. Baerends (2003). *J. Comp. Chem.* **24**, 1142.
26. E. J. Baerends, D. E. Ellis, and P. Ros (1973). *Chem. Phys.* **2**, 42.
27. E. van Lenthe, E. J. Baerends, and J. G. Snijders (1993). *J. Chem. Phys.* **99**, 4597.
28. B. Kesanli, J. Fettinger, and B. Eichhorn (2001). *Chem. Eur. J.* **7**, 5277.
29. J. Campbell, H. P. A. Mercier, F. Holger, D. Santry, D. A. Dixon, and G. J. Schrobilgen (2002). *Inorg. Chem.* **41**, 86.
30. J. M. Goicoechea and S. C. Sevov (2006). *Organometallics* **25**, 4530.
31. B. B. Zhou, M. S. Denning, C. Jones, J. M. Goicoechea (2009) Dalton Trans. 1571.
32. J. M. Goicoechea and S. C. Sevov (2006). *J. Am. Chem. Soc.* **128**, 4155.
33. E. N. Esenturk, J. Fettinger, and B. Eichhorn (2006). *Polyhedron* **25**, 521.
34. B. Kesanli, J. Fettinger, D. R. Gardner, and B. Eichhorn (2002). *J. Am. Chem. Soc.* **124**, 4779.
35. K. Wade (1971) J. Chem. Soc., Chem. Commun. 792.